







Multimodal mechanisms of human socially reinforced learning across neurodegenerative diseases

Agustina Legaz,^{1,2,3}  Sofía Abrevaya,^{2,4} Martín Dottori,¹ Cecilia González Campo,^{1,2} Agustina Birba,^{1,2} Miguel Martorell Caro,^{2,4} Julieta Aguirre,⁵ Andrea Slachevsky,^{6,7,8,9} Rafael Aranguiz,¹⁰ Cecilia Serrano,¹¹ Claire M. Gillan,^{12,13,14,15} Iracema Leroi,^{12,15}  Adolfo M. García,^{1,2,12,15,16,17}  Sol Fittipaldi^{1,2,3} and  Agustín Ibañez^{1,2,12,15,18}

Social feedback can selectively enhance learning in diverse domains. Relevant neurocognitive mechanisms have been studied mainly in healthy persons, yielding correlational findings. Neurodegenerative lesion models, coupled with multimodal brain measures, can complement standard approaches by revealing direct multidimensional correlates of the phenomenon.

To this end, we assessed socially reinforced and non-socially reinforced learning in 40 healthy participants as well as persons with behavioural variant frontotemporal dementia ($n = 21$), Parkinson's disease ($n = 31$) and Alzheimer's disease ($n = 20$). These conditions are typified by predominant deficits in social cognition, feedback-based learning and associative learning, respectively, although all three domains may be partly compromised in the other conditions. We combined a validated behavioural task with ongoing EEG signatures of implicit learning (medial frontal negativity) and offline MRI measures (voxel-based morphometry).

In healthy participants, learning was facilitated by social feedback relative to non-social feedback. In comparison with controls, this effect was specifically impaired in behavioural variant frontotemporal dementia and Parkinson's disease, while unspecific learning deficits (across social and non-social conditions) were observed in Alzheimer's disease. EEG results showed increased medial frontal negativity in healthy controls during social feedback and learning. Such a modulation was selectively disrupted in behavioural variant frontotemporal dementia. Neuroanatomical results revealed extended temporo-parietal and fronto-limbic correlates of socially reinforced learning, with specific temporo-parietal associations in behavioural variant frontotemporal dementia and predominantly fronto-limbic regions in Alzheimer's disease. In contrast, non-socially reinforced learning was consistently linked to medial temporal/hippocampal regions. No associations with cortical volume were found in Parkinson's disease. Results are consistent with core social deficits in behavioural variant frontotemporal dementia, subtle disruptions in ongoing feedback-mechanisms and social processes in Parkinson's disease and generalized learning alterations in Alzheimer's disease. This multimodal approach highlights the impact of different neurodegenerative profiles on learning and social feedback.

Our findings inform a promising theoretical and clinical agenda in the fields of social learning, socially reinforced learning and neurodegeneration.

- 1 Cognitive Neuroscience Center, Universidad de San Andrés, Buenos Aires C1011ACC, Argentina
- 2 National Scientific and Technical Research Council (CONICET), Buenos Aires C1425FQB, Argentina
- 3 Facultad de Psicología, Universidad Nacional de Córdoba, Córdoba CU320, Argentina
- 4 Institute of Cognitive and Translational Neuroscience, INECO Foundation, Favaloro University, CONICET, Buenos Aires C1021, Argentina

Received June 15, 2021. Revised August 17, 2021. Accepted September 06, 2021. Advance access publication September 16, 2021

© The Author(s) (2021). Published by Oxford University Press on behalf of the Guarantors of Brain.

This is an Open Access article distributed under the terms of the Creative Commons Attribution-NonCommercial License (<https://creativecommons.org/licenses/by-nc/4.0/>), which permits non-commercial re-use, distribution, and reproduction in any medium, provided the original work is properly cited. For commercial re-use, please contact journals.permissions@oup.com

- 5 Instituto de Investigaciones Psicológicas (IIPsi), CONICET, Universidad Nacional de Córdoba, Córdoba CB5000, Argentina
- 6 Memory and Neuropsychiatric Clinic (CMYN) Neurology Department, Hospital del Salvador, SSMO & Faculty of Medicine, University of Chile, Santiago, Chile
- 7 Neurology Department, Gerosciences Center for Brain Health and Metabolism (GERO), Santiago, Chile
- 8 Neuropsychology and Clinical Neuroscience Laboratory, Physiopathology Department, ICBM, Neurosciences Department, Faculty of Medicine, University of Chile, Chile
- 9 Servicio de Neurología, Departamento de Medicina, Clínica Alemana-Universidad del Desarrollo, Chile
- 10 Unidad de Neuropsicogeriatría, Instituto Nacional de Geriatría, Santiago, Chile
- 11 Unidad de Neurología Cognitiva, Hospital César Milstein, Buenos Aires C1221, Argentina
- 12 Global Brain Health Institute, University of California San Francisco, San Francisco, CA 94158, USA
- 13 Department of Psychology, Trinity College Dublin, Dublin, Ireland
- 14 Trinity College Institute of Neuroscience, Trinity College Dublin, Dublin, Ireland
- 15 Global Brain Health Institute, Trinity College Dublin, Dublin Dublin 2, Ireland
- 16 Faculty of Education, National University of Cuyo, Mendoza M5502JMA, Argentina
- 17 Departamento de Lingüística y Literatura, Facultad de Humanidades, Universidad de Santiago de Chile, Santiago, Chile
- 18 Latin American Brain Health Institute (BrainLat), Universidad Adolfo Ibáñez, Santiago, Chile

Correspondence to: Sol Fittipaldi
 Centro de Neurociencias Cognitivas and CONICET; Vito Dumas 284
 B1644BID Victoria, Buenos Aires, Argentina
 E-mail: fittipaldisol@gmail.com

Correspondence may also be addressed to: Agustín Ibáñez
 E-mail: agustin.ibanez@gbhi.org

Keywords: learning; social reinforcement; behavioural variant frontotemporal dementia; Alzheimer's disease; Parkinson's disease

Abbreviations: bvFTD = behavioural variant frontotemporal dementia; MFN = medial frontal negativity; (N)SRL = (non)-socially reinforced learning

Introduction

Social reinforcement is a powerful facilitator of learning,^{1–4} especially relative to non-social feedback.^{5–10} Contextual interpersonal cues like facial emotional expressions^{11,12} promote associative learning^{10,13} by engaging emotional arousal and reward/punishment mechanisms.^{14–16} According to the social-context network model, these integrative processes implicate a broad fronto-insulo-temporal network,^{17–22} with socially reinforced learning (SRL) depending critically on temporo-parietal hubs and secondarily on fronto-limbic hubs, both related to context-target associative learning and social cognition.^{20,21,23–27} However, most evidence comes from healthy individuals, offering limited (correlational) information to identify critical neural signatures. The neurodegenerative lesion model approach partially overcomes these limitations by revealing direct links between affected brain mechanisms and behavioural performance.^{28–32} Yet, while some works have examined social versus non-social learning in neurodegenerative diseases (Table 1),^{33,34} and others have addressed SRL through neurophysiological methods,^{25,26,35} no study has integrated both approaches—let alone with a multimodal framework. Here, we examined behavioural, EEG and structural neuroimaging correlates of an SRL paradigm in healthy controls as well as patients with behavioural variant frontotemporal dementia (bvFTD), Parkinson's disease and Alzheimer's disease, typified by predominant deficits in social cognition, feedback-based learning and associative learning, respectively.

Preliminary psychophysiological evidence (behavioural and EEG studies) points to different patterns of disturbance across

neurodegenerative subtypes. In bvFTD, impaired processing of socially relevant information^{36,37} is particularly evident in associative learning tasks.^{33,36} Such deficits have been linked to disruptions of social reward processing^{36,38} and contextual integration skills.^{18,39,40} In Parkinson's disease, although impaired feedback-based learning has been reported,^{41–43} no study has compared performance in social and non-social feedback conditions, despite reported socioemotional disturbances in this disease.^{44–46} In Alzheimer's disease, although socioemotional functions usually remain partially intact in mild-moderate stages,^{47,48} facial cues do not enhance associative learning^{33,36} (but see Duff et al.³⁴). Altogether, beyond reported overlapping disruptions in memory and social cognition domains across neurodegenerative conditions,^{47,49–51} behavioural evidence points to predominately sociocontextual learning impairments in bvFTD, implicit learning and socioemotional disturbances in Parkinson's disease and general learning deficits in Alzheimer's disease. Finally, EEG evidence of SRL is limited in neurodegenerative conditions. While social processing impairments have been related to diminished frontal EEG activity in bvFTD,⁴⁰ no previous work has associated SRL with ongoing EEG activity in other neurodegenerative diseases.

Neuroimaging evidence of SRL is also scant. In bvFTD, social learning impairments have been related to orbitofrontal and temporal grey matter atrophy.³⁶ With regards to Parkinson's disease, although a link between feedback-based learning impairments and cortico-striatal dysfunctions has been assumed,^{41,43} no previous work has directly examined structural associations

with SRL in this group. Finally, in Alzheimer's disease, disrupted social enhancement in associative learning has been related to medial temporal and parietal atrophy.^{6,36,52}

Although social and feedback-based learning have been separately assessed in bvFTD, Parkinson's disease and Alzheimer's disease (Table 1), no previous work has jointly addressed SRL in neurodegenerative models that differentially impact social cognition, feedback-based learning and general associative learning. To our knowledge, this is the first feedback-based associative learning study combining social and non-social cues in neurodegeneration. Moreover, no previous work has targeted SRL/non-socially reinforced learning (NSRL) while tracking ongoing EEG correlates in different neurodegenerative groups—let alone in a multidimensional approach combining behavioural, EEG and neuroimaging.

Our approach enables the joint assessment of feedback-related mechanisms across behavioural, neurophysiological and neuro-anatomical dimensions. We adapted an associative learning paradigm, previously reported with healthy participants,¹⁰ that evaluates how social and non-social feedback impacts implicit learning of an arbitrary association between two stimulus types. Specifically, the task requires participants to judge the category membership ('A' or 'B') of repeatedly presented three-digit numbers, and learn (across different cycles) the correct association upon receiving feedback via socioemotional facial expressions (SRL) or coloured circles (NSRL) after each number–category judgement. Learning is indexed by increased accuracy and/or response time across cycles. High-density EEG allowed tracking ongoing markers of feedback-based learning via medial frontal negativity (MFN) modulations,^{53–55} a group of event-related potentials (error-related negativity, feedback-related negativity and N2) sensitive to cognitive demands and strategic on-the-fly adjustments.^{54,55} Specifically, larger MFN is predictive of enhanced learning by feedback.^{53,56,57} Moreover, MRI recordings were obtained offline to investigate neuroanatomical correlates of SRL.

In healthy controls, we predicted enhanced performance across the task (final > initial trials), with better performance after social relative to non-social feedback (SRL > NSRL).^{10,13} Similarly, we expected that both effects would be associated with larger MFN.^{53,56–58} Also, in line with the social-context network model, we predicted that SRL performance would be related with extended temporo-posterior (and, to a lesser degree, frontal) regions involved in sociocontextual processing and learning.^{20,21,24,25} Conversely, we anticipated that NSRL would be associated with regions underpinning associative learning (i.e. hippocampal and medial temporal lobe structures).^{6,59}

Furthermore, in comparison with controls, distinct SRL disruptions were predicted for each neurodegenerative group. In bvFTD, due to its well-known social processing impairments, we expected reduced social-feedback facilitation on behavioural performance, alongside diminished MFN modulations for SRL relative to NSRL, as well as brain–behaviour associations across temporo-posterior regions in (impaired) SRL and hippocampal regions in (preserved) NSRL. In Parkinson's disease, considering prominent feedback-related learning and socioemotional disturbances, we predicted behavioural SRL deficits and impaired MFN modulations during final trials. Regarding Alzheimer's disease, we hypothesized behavioural impairments in both feedback conditions (SRL and NSRL), along with diminished MFN modulations during final trials (in contrast to healthy controls), resembling generalized learning deficits, associated with temporo-posterior atrophy. By jointly testing these hypotheses, we aim to provide convergent multimodal evidence of SRL disruptions across neurodegenerative diseases.

Materials and methods

Participants

The study comprised 112 participants: 40 healthy controls with preserved cognition and no history of neuropsychiatric diseases and/or substance abuse; 21 individuals fulfilling revised criteria for bvFTD⁶⁰; 31 patients with Parkinson's disease diagnosed in accordance with the United Kingdom Parkinson's Disease Society Brain Bank criteria⁶¹; and 20 patients with Alzheimer's disease, each fulfilling the international National Institute of Neurological and Communicative Disorders and Stroke–Alzheimer's Disease and Related Disorders Association (NINCDS-ARDA) criteria.^{62,63} Power analyses confirmed the adequacy of our sample size (Supplementary material). Participants were recruited from three international clinics taking part in the Multi-Partner Consortium to Expand Dementia Research in Latin America (ReDLat)^{64,65} and assessed following harmonized procedures^{64,65} as in previous works.^{32,40,66–70} Clinical diagnoses were established by neurodegenerative disease experts through an extensive neurological, neuropsychiatric and neuropsychological examination comprising semistructured interviews and standardized cognitive and functional assessments (Table 2 and Supplementary material). All participants with neurodegenerative conditions were in early/mild stages of the disease and did not fulfil criteria for other neurological disorders or specific psychiatric conditions; neither did they present primary language deficits or a history of substance abuse. Participants with bvFTD were functionally impaired and exhibited prominent changes in personality and social behaviour, as verified by caregivers. Participants with Parkinson's disease were medicated with antiparkinsonian therapy and evaluated during 'on' phase. Participants with Alzheimer's disease were also functionally impaired, as verified by caregivers. Each neurodegenerative sample was comparable in sex, age and years of formal education with healthy controls. The only significant difference in sex between bvFTD and healthy controls (Table 2) was controlled in all subsequent analyses. Finally, whole-brain grey matter was compared between each neurodegenerative group and healthy controls, showing a predominantly orbitofronto-cingulate-temporal atrophy in bvFTD,^{18,71,72} no atrophy in Parkinson's disease^{73–75} and extended bilateral temporal with less extended fronto-parietal atrophy in Alzheimer's disease^{76–78} (Supplementary Fig. 1 and Supplementary material). The institutional ethics committee of each recruitment centre approved the study protocol. All participants provided signed informed consent in accordance with the Declaration of Helsinki.

Experimental protocol

All participants completed a multimodal assessment protocol including a behavioural SRL assessment, ongoing high-density EEG recordings and an MRI session.

Behavioural data: socially reinforced learning task

We adapted an SRL task validated in a behavioural study with healthy persons.¹⁰ By pressing predefined keys, participants were asked to judge the category membership 'A' or 'B' of three-digit numbers presented repeatedly across six cycles on a computer screen. Visual feedback immediately followed each number–category judgement (Fig. 1A). Participants were informed that there was no underlying rule defining the category membership of each number. Knowledge of the correct or incorrect outcome of previous category judgements for a particular number served to enhance performance over subsequent cycles. The task comprised two feedback conditions. In the SRL condition, socioemotional

Table 1 Previous studies that assessed social learning and feedback-based learning in behavioural variant frontotemporal dementia, Alzheimer’s disease, and/or Parkinson’s disease

Authors/journal	Groups: n	Tasks	Behavioural performance	Social information improves learning?	EEG, brain structural and/or functional associations
Keri ³³ Cortex	Early-stage bvFTD: 16, elderly, early-stage Alzheimer’s disease: 20, HCs: 20	Paired-associate learning task: real-life game (real persons) (social) versus computer games (boxes and neutral faces) (non-social)	Real-life game: HCs = Alzheimer’s disease > bvFTD Computer games: HCs = bvFTD > Alzheimer’s disease	Yes, only real-life interactions improved associative learning in early-stage Alzheimer’s disease	NA
Wong et al. ³⁶ Neuropsychologia	bvFTD: 20, Alzheimer’s disease: 14, HCs: 20	Trust game task: steal/share associated to face (social) versus lottery (non-social)	Social learning accuracy: HCs > bvFTD = Alzheimer’s disease	No, reduced capacity to learn socially relevant information in both bvFTD and Alzheimer’s disease	GM atrophy (VBM) correlations for bvFTD (lateral occipital cortex, superior temporal gyrus, middle temporal gyrus, frontal pole, orbitofrontal cortex, putamen, middle frontal gyrus) and for Alzheimer’s disease (superior temporal gyrus, cerebellum, parahippocampal gyrus, hippocampus, lateral occipital cortex)
Duff et al. ³⁴ The Journal of Comparative Neurology	Early-stage Alzheimer’s disease: 5, HCs: 10	Collaborative referencing task (real-life interactive learning task) (social) versus paired-associate learning control task (non-social)	Collaborative referencing task: HCs = Alzheimer’s disease Paired-associate learning control task: HCs > Alzheimer’s disease	Yes, real-life interactions with a familiar person improved associative learning in early-stage Alzheimer’s disease	NA
Schmitt-Ehassen et al. ⁴² Brain Research	Parkinson’s disease: 31, elderly HCs: 30	Feedback-based learning task versus observational learning task (only non-social)	Feedback-based task: HCs = Parkinson’s disease (but no learning effect under feedback-based task compared to observational task in either group)	NA	NA
Meissner et al. ⁴¹ Behavioural Brain Research	Parkinson’s disease: 18, HCs: 18	Feedback-based learning task (only non-social)	Feedback-based task: HCs > Parkinson’s disease	NA	NA
Shohamy et al. ⁴³ Brain	Parkinson’s disease: 13, HCs: 13	Feedback-based learning task versus observational learning task (only non-social)	Feedback-based task: HCs > Parkinson’s disease Observational task: HCs = Parkinson’s disease	NA	NA

HCs = healthy controls; GM = grey matter; VBM = voxel-based morphometry.

Table 2 Samples' demographic and neuropsychological data

	HCs (n = 40)	bvFTD (n = 21)	Parkinson's disease (n = 31)	Alzheimer's disease (n = 20)	Stats	Post hoc comparisons
Demographics						
Sex** (M: F)	18:22	16:05	18:13	9:11	$\chi^2 = 6.32$ $P = 0.09$	HC–bvFTD: $P = 0.02^*$ HC–Parkinson's disease: $P = 0.27$ HC–Alzheimer's disease: $P = 1$
Age**	68.92 (8.66)	66.67 (11.52)	70.48 (9.10)	73.00 (6.01)	$F = 1.86$ $P = 0.13$ $\eta_p^2 = 0.04$	HC–bvFTD: $P = 0.35$ HC–Parkinson's disease: $P = 0.47$ HC–Alzheimer's disease: $P = 0.10$
Education	13.90 (3.67)	14.43 (5.03)	12.29 (4.31)	12.30 (4.00)	$F = 1.76$ $P = 0.15$ $\eta_p^2 = 0.04$	HC–bvFTD: $P = 0.64$ HC–Parkinson's disease: $P = 0.11$ HC–Alzheimer's disease: $P = 0.16$
Handedness (R:L)	38:2	20:1	29:2	19:1	–	–
Cognitive assessment						
MoCA**	25.59 (2.57)	21.00 (5.51)	21.93 (4.31)	16.11 (4.46)	$F = 24.14$ $P < 0.001^*$ $\eta_p^2 = 0.40$	HC–bvFTD: $P < 0.001^*$ HC–Parkinson's disease: $P < 0.001^*$ HC–Alzheimer's disease: $P < 0.001^*$
IFS**	22.09 (3.79)	18.62 (6.30)	19.88 (4.12)	14.97 (4.38)	$F = 11.30$ $P < 0.001^*$ $\eta_p^2 = 0.24$	HC–bvFTD: $P = 0.006^*$ HC–Parkinson's disease: $P = 0.05$ HC–Alzheimer's disease: $P < 0.001^*$

Results are presented as mean (SD). Lower executive function scores (IFS) in Alzheimer's disease are triggered by advanced age and lower general cognitive state.¹⁶² Demographic and cognitive data were assessed through ANOVAs and post hoc pairwise comparisons—except for sex, which was analysed via Pearson's chi-squared (χ^2) test. Effects sizes were calculated through partial eta (η_p^2). HCs: healthy controls; IFS = INECO Frontal Screening¹⁶³; MoCA = Montreal Cognitive Assessment.¹⁶⁴

*Significant differences with an alpha level of $P < 0.05$.

**Variables with significant differences ($P < 0.05$) between neurodegenerative groups, precluding comparisons between them in our target measures.

feedback was given a single face with one smiling and one angry expression for correct and incorrect responses, respectively.¹⁰ The faces' gender matched the participant's gender. In the NSRL condition, feedback was given via green and red circles displayed for correct and incorrect responses, respectively. At the end of the experiment, participants were explicitly asked about the valence of each feedback type (Table 3). All groups presented adequate comprehension of these two factors (with no significant differences; for details see [Supplementary material](#)). Each trial consisted of an initial stimulus (a three-digit number) presented in white colour over a black background for 1500 ms, followed by a black screen (1000 ms) and then by categories' options ('A' and 'B') positioned to the left and right of the screen over left/right arrows, respectively. Participants had to respond by choosing a letter through the corresponding computer keyboard arrows with their dominant hand. Afterwards, another black screen was shown for a random period (between 2000 and 2500 ms). Finally, social or non-social feedback was provided for 1000 ms. Instructions and a set of two practice trials were presented before each block. The order of SRL/NSRL blocks alternated, with the first being social for half of the participants. Categories A or B were counterbalanced in a pseudorandom design across blocks. In total, participants completed six blocks (three SRL, three NSRL). Four different three-digit numbers (four trials) were repeated across six cycles per block. In total, 24 different numerical stimuli and 144 trials were run per subject. The number of trials did not change according to performance. For further details on the task design see [Supplementary material](#). Accuracy and response time data were collected for each trial. During the whole task, high-density EEG recordings were obtained to assess potential electrophysiological differences between SRL and NSRL modulations across groups (see below).

EEG acquisition and signal preprocessing

Signals were acquired, for all participants, with a Biosemi Active-two 128-channel system at 1024 Hz. Data were re-referenced

offline separately to linked mastoid electrodes, resampled at 512 Hz and filtered at 0.5–50 μ V. Eye movements or blink artefacts were corrected with independent component analysis⁷⁹ and with a visual inspection protocol.^{30,32,80–87} Noisy epochs were rejected using an automatic EEGLAB procedure. Criteria for exclusion included elimination of trials that exceeded a threshold of 2.5 SDs from the mean probability distribution calculated from all trials and by measuring the kurtosis of probability distribution.⁸⁸ The percentage of rejected trials was similar across groups and conditions ([Supplementary Tables 5.1 and 5.2](#)). EEG data were segmented into 1-s epochs and baseline-corrected (–200 to 0 ms) for the feedback stimuli.

Neuroimaging acquisition and preprocessing

MRI acquisition and pre-processing steps are reported as recommended by the Organization for Human Brain Mapping.^{89,90} Acquisition parameters in each centre followed standard protocols^{30,32,91} ([Supplementary material](#)). For neuroanatomical analysis, whole-brain T₁-rapid anatomical three-dimensional gradient echo volumes were acquired. Sixteen three-dimensional volumetric images (from six healthy controls, three bvFTD, five Parkinson's disease and two Alzheimer's disease participants) were excluded due to missing or artefactual data. The resulting subsamples were demographically matched in age and years of formal education. However, as regards sex, a significant difference was observed between bvFTD and healthy controls ([Supplementary Table 6.2](#)). These differences were controlled in the statistical analyses (see 'Statistical analysis' section).

For voxel-based morphometry (VBM) analysis, data were processed on the DARTEL Toolbox following validated procedures^{30,66,92} via Statistical Parametric Mapping software (SPM12, <https://www.fil.ion.ucl.ac.uk/spm/software/spm12/>; accessed 9 February 2022). T₁-weighted images in native space were first segmented using the default parameters of the SPM12 (bias regularization was set to 0.001 and bias full-width at half-maximum

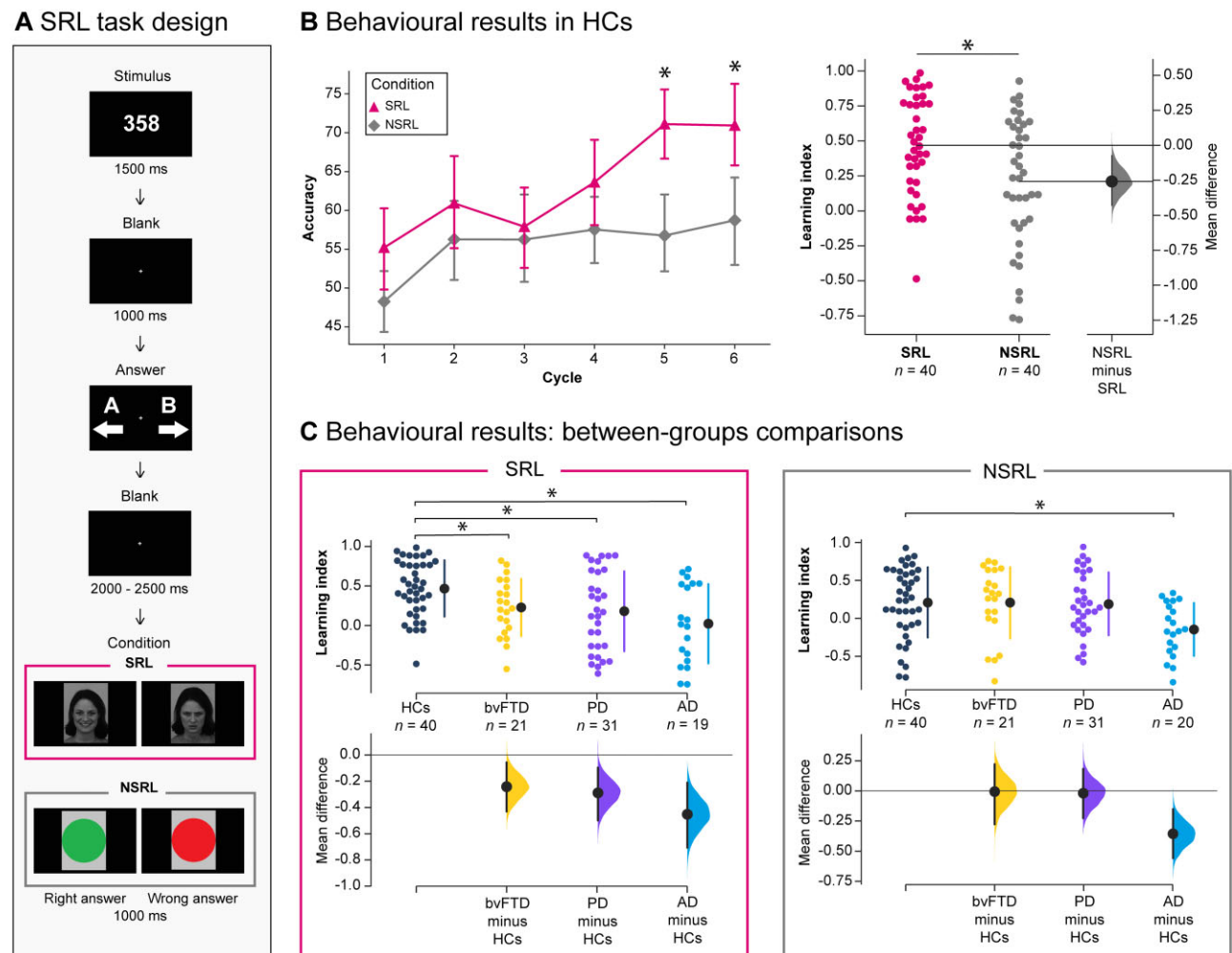


Figure 1 SRL task and behavioural results. (A) SRL task design. Participants judged whether three-digit numbers presented repeatedly on a computer screen belonged to either category ‘A’ or ‘B’. Visual feedback immediately followed each number–category judgement (smiling face for correct responses or angry face for incorrect responses in the SRL condition; green circle for correct responses or red circle for incorrect responses in the NSRL condition). High-density EEG recordings were obtained during the task. (B) Behavioural results in healthy controls. *Left*: Repeated-measures ANOVA of accuracy across cycles and feedback conditions. *Right*: One-way ANOVA between feedback conditions for the learning index (Spearman’s rank correlation coefficient values for the accuracy score by cycle). The mean difference (effect size) of the between-conditions comparison in healthy controls (NSRL minus SRL) is reported. (C) Behavioural results: between-group comparisons. Learning index for comparisons of behavioural performance between groups, for SRL and NSRL conditions. The between-groups mean difference (effect size) between healthy controls and each neurodegenerative group is reported below each result. Behavioural results were replicated when controlling for sex and valence recognition (Supplementary material). The asterisk (*) indicates significant differences with an alpha of $P < 0.05$. AD = Alzheimer’s disease; HCs = healthy controls; PD = Parkinson’s disease.

Table 3 Feedback valence ratings

Feedback accuracy	HCs (n = 40)	bvFTD (n = 21)	Parkinson’s disease (n = 31)	Alzheimer’s disease (n = 20)
Total	0.94 (0.24)	0.88 (0.33)	0.80 (0.4)	0.81 (0.39)
Social	0.90 (0.30)	0.92 (0.27)	0.81 (0.40)	0.85 (0.36)
Non-social	0.98 (0.16)	0.82 (0.38)	0.79 (0.41)	0.78 (0.42)
Social positive	0.90 (0.30)	1 (0)	0.81 (0.40)	0.85 (0.37)
Social negative	0.90 (0.30)	0.85 (0.37)	0.81 (0.40)	0.85 (0.37)
Non-social positive	0.98 (0.16)	0.90 (0.31)	0.84 (0.37)	0.85 (0.37)
Non-social negative	0.98 (0.16)	0.75 (0.44)	0.74 (0.44)	0.70 (0.47)

Results are presented as mean (SD). To assess feedback valence recognition among groups, participants were explicitly asked about the valence (positive, negative) of each feedback type [Social (smiling face, angry face); non-social (green circle, red circle)] at the end of the experiment. All groups presented adequate valence recognition (with no significant differences; for details see Supplementary material). HCs = healthy controls.

(FWHM) was set to 60-mm cut-off) into grey matter, white matter and CSF (these three tissues were used to estimate the total intracranial volume). DARTEL (create template) module was run later using the grey matter and white matter segmented images—following SPM12 default parameters—to create a template that is generated from the complete dataset (increasing the accuracy of intersubject alignment).⁹³ Next, we used the ‘Normalize to MNI Space’ module from DARTEL Tools to affine register the last template from the previous step into the MNI Space. This transformation was applied to all the individual grey matter segmented scans to also be brought into standard space. Subsequently, all images were modulated to correct volume changes by Jacobian determinants and to avoid bias in the intensity of an area due to its expansion during warping. Finally, data were smoothed using a 10-mm FWHM isotropic Gaussian kernel to accommodate for intersubject differences in anatomy. The size of the kernel was selected based on previous recommendations.^{92,94}

To analyse the images of each centre together and avoid a scanner effect in our results, the normalized and smoothed DARTEL outputs were transformed to *w*-score images.^{95–99} *w*-Scores, similar to *z*-scores (mean = 0, SD = 1), represent the degree to which the observed grey matter volume in each voxel is higher or lower (positive or negative *w*-score) than expected, based on an individuals’ global composite score adjusted for specific covariates (age, disease, total intracranial volume and scanner type). *w*-Scores were calculated dividing each participant’s observed and predicted grey matter volume (residuals) by their SD. The resulting *w*-score maps of each subject were used for further statistical analyses.

Statistical analysis

Behavioural analysis: socially reinforced learning task

First, we discarded trials with response latencies above 10 s (for details see [Supplementary material](#)). Second, we excluded trials whose response time fell more than 3 SDs away from each subject’s mean.¹⁰⁰ The percentage of rejected trials was similar across groups and conditions ([Supplementary Table 3.2](#)). To validate the results in healthy controls, accuracy scores (the number of correct responses per cycle and per feedback condition) were calculated for each subject. To confirm the expected effect of learning (higher accuracy over successive cycles) and feedback type (higher accuracy in SRL than in NSRL condition) in healthy controls, we analysed their performance through repeated-measures ANOVA of accuracy scores across cycles and feedback condition. A Shapiro–Wilk test for normality on healthy controls’ accuracy evidenced normal distribution ([Supplementary material](#)).

For each subject, we computed a learning index calculated as the rho value of the Spearman correlation between accuracy and cycle number.^{101–103} We obtained one learning index for each SRL and NSRL condition. This measure integrates the accuracy-by-cycle interaction in a slope index, allowing us to compare the learning process between conditions.¹⁰¹ Performance was compared between feedback conditions via a one-way ANOVA for the learning index in healthy controls.

Next, the following procedure was designed to compare healthy controls and patients. To compare behavioural performance between groups, as normality and homoscedasticity assumptions were not fully met ([Supplementary material](#)), non-parametric Kruskal–Wallis tests were conducted for the learning index (with two-tail Mann–Whitney U-tests for *post hoc* comparisons). As in previous reports with neurodegenerative diseases,^{30,32,104–106} because our hypotheses hinged on differences between each neurodegenerative group and healthy controls, and given that demographic and behavioural features were not

matched across neurodegenerative samples (bvFTD versus Parkinson’s disease versus Alzheimer’s disease), we focused on pairwise comparisons between demographically matched tandems: healthy controls versus bvFTD, healthy controls versus Parkinson’s disease, healthy controls versus Alzheimer’s disease ([Table 2](#)). In addition, given that a significant difference was found in sex between bvFTD and healthy controls, we conducted additional group comparison analyses of covariance using permutation testing controlling for sex¹⁰⁷ ([Supplementary material](#)). Moreover, to rule out potential confounds of facial emotion recognition disturbances in bvFTD (particularly, for negative emotions),^{108,109} we also conducted additional group comparison analyses of covariance using permutation testing and controlling for feedback valence recognition ([Supplementary material](#)). Finally, we carried out modified *t*-tests¹¹⁰ to estimate the percentage of impaired learning indexes in participants with neurodegenerative disease in contrast to healthy controls. This analysis allows assessment of the percentage of cases that met criteria for dissociation between SRL and NSRL conditions (see [Supplementary material](#) for details).

EEG: spatiotemporal clustering associated to feedback

To track ongoing markers of learning by feedback we targeted the MFN, characterized by a negative deflection over the midline frontal region of the scalp.^{53–55} Here, we aimed to analyse the potential differences in MFN modulations of SRL versus NSRL by comparing the spatiotemporal cluster for both feedback conditions for each group. Also, in order to assess early versus late learning modulation effects of ongoing MFN markers, we included an additional measure (initial versus final set of trials), as previously done.¹¹¹ We compared the initial (first half) versus final (second half) set of trials per cycle of the social condition within each group. We used a split analysis applying the same MFN approach as it represents a direct measure of learning by feedback. The learning index is a dimensional measure of the slope of the behavioural correlation and does not directly represent an association with the MFN modulation by feedback. This way, we avoided problems related to (i) the rho not being univariate; (ii) inflating the number of comparisons between time points and electrodes due to single-trial analysis in a regression; and (iii) controversial single-trial association between performance and event-related potential given the high level of noise,¹¹² as signal averaging approaches are less affected by artefacts and noise-related variability.¹¹³ Given these considerations, and following similar approaches performed with the MFN^{111,114} and other event-related potentials,^{115,116} we evaluated the learning effects using a MFN split analysis.

To avoid a *a priori* spatiotemporal bias, non-parametric data-driven spatiotemporal clustering¹¹⁷ was implemented on Matlab software with the Fieldtrip Toolbox (version 20180313), with one-tailed paired *t*-tests as univariate tests. This non-parametric clustering method was introduced to address the resulting multiple comparisons problem.¹¹⁸ The *t*-values of adjacent spatiotemporal points with $P < 0.05$ were clustered together by summing their *t*-values, and the largest cluster was retained. A minimum of 10 neighbouring electrodes were required to pass this threshold and form a robust cluster.¹¹⁹ The cluster-level *t*-value was calculated as the sum of the individual *t*-values at the points within the cluster. To assess the significance of a spatiotemporal cluster identified above, this procedure was repeated 5000 times, with recombination and randomized resampling of the subject-wise averages before each repetition using a Monte Carlo method.¹²⁰ After each repetition, the *t*-value of the largest cluster identified was retained. The proportion of these 5000 randomized *t*-values greater than the originally identified cluster-level *t*-value was used to calculate a

non-parametric *P* value for the originally identified cluster. This approach avoids the problem of multiple comparisons across the dimensions of electrode, time and space.^{117,119}

Neuroimaging: voxel-based morphometry analysis

Regression analyses were performed to assess the association between grey matter volume and behavioural performance (SRL and NSRL learning indexes) via non-parametric permutation tests on Statistical non-parametric Mapping [SnPM13, <http://www.nisox.org/Software/SnPM13/> (accessed 9 February 2022), 5000 random permutations, cluster-forming threshold set at 0.001] toolbox for SPM12. Permutation tests outperform parametric tests in correction for multiple comparisons.¹²¹ Sex was included as a covariate of no interest. In order to increase behavioural variance and statistical power by increasing sample size,^{39,122–124} we used two approaches collapsing different groups. First, we performed analyses including all four groups (healthy controls, bvFTD, Parkinson's disease and Alzheimer's disease), to assess a general association between brain correlates of performance. Second, each pathological group was analysed in tandem with healthy controls (bvFTD–healthy controls, Parkinson's disease–healthy controls and Alzheimer's disease–healthy controls) to evaluate specific performance-related neuroanatomical correlates, following recent neurodegenerative studies.^{30,32,125–128} To adjust for multiple comparisons, we used cluster-wise inference with family-wise error (FWE) rate correction of $P\text{-FWE} < 0.05$.^{129,130} Finally, a conjunction analysis was performed in order to assess the extent of shared/distinct neural correlates of SRL and NSRL conditions. We used Imcalc in SPM12, to assess the conjoint analysis of grey matter volume and the two learning indexes in all groups together with corrected thresholded maps ($P\text{-FWE} < 0.05$). The binarized images were used to obtain a conjunction map using the equation: $i1 + (2 \times i2)$.^{131,132}

Data availability

Anonymized data that support the study findings are available in open-source software¹³³ or from the corresponding author upon reasonable request.

Table 4 Statistical comparison between groups (healthy controls, bvFTD, Parkinson's disease and Alzheimer's disease) and conditions (SRL and NSRL) in the learning index

Kruskal–Wallis test							
Condition	HCs	bvFTD	Parkinson's disease	Alzheimer's disease	Statistical results		
					<i>H</i>	<i>P</i>	$\eta^2[H]$
SRL	0.46 (0.35)	0.22 (0.35)	0.17 (0.49)	0.007 (0.48)	13.54	0.003*	0.097
NSRL	0.21 (0.45)	0.20 (0.45)	0.19 (0.40)	−0.14 (0.33)	10.89	0.01*	0.073
Mann–Whitney U							
Condition	HCs	Neurodegenerative samples	Statistical results				
			<i>U</i>	<i>P</i>	Cohen's <i>d</i>		
SRL	0.46 (0.35)	bvFTD: 0.22 (0.35)	577	0.017*	0.641		
		Parkinson's disease: 0.17 (0.49)	830.5	0.014*	0.605		
		Alzheimer's disease: 0.007 (0.48)	186	0.001*	0.961		
NSRL	0.21 (0.45)	bvFTD: 0.20 (0.45)	419.5	0.997	0.002		
		Parkinson's disease: 0.19 (0.40)	655.5	0.684	0.098		
		Alzheimer's disease: −0.14 (0.33)	210.5	0.003*	0.831		

Results are presented as mean (SD). The asterisk (*) indicates significant differences with an alpha level of $P < 0.05$. Learning Index (Spearman correlation's rho slope of cycles and accuracy score) was assessed through non-parametric Kruskal–Wallis tests (with two-tail Mann–Whitney *U* tests for *post hoc* comparisons). Effect size for the Kruskal–Wallis test was calculated as the eta-squared based on the *H*-statistic: $(H - k + 1)/(n - k)$, *k* being the number of groups, and for the Mann–Whitney *U* the Cohen's *d* value was obtained.¹⁶³ bvFTD = behavioural variant of fronto-temporal dementia; HCs = healthy controls.

Results

Behavioural results

In healthy controls, accuracy improved across cycles, even when assessing SRL and NSRL conditions separately. Moreover, accuracy was higher in the SRL than in the NSRL condition (Fig. 1B and Supplementary material). In this line, performance was also compared between feedback conditions for the learning index, revealing a significant difference between SRL (mean = 0.47, SD = 0.36) and NSRL (mean = 0.21, SD = 0.46) feedback conditions [$F(1,39) = 8.49$, $P = 0.005$, $\eta_p^2 = 0.17$; Fig. 1B] in healthy controls.

Moreover, the learning index was used to assess between-group comparisons. A significant main effect of group was observed for the learning index in SRL and in NSRL conditions (Table 4).

When comparing the learning index between each neurodegenerative sample and healthy controls separately, we found that participants with bvFTD performed significantly worse in the SRL condition, but not in the NSRL condition. The same pattern was observed in participants with Parkinson's disease. Finally, Alzheimer's disease showed impaired learning in both conditions relative to healthy controls (Table 4 and Fig. 1C). Behavioural results were replicated when controlling for sex (see Supplementary Material 3.5) and valence recognition (see Supplementary Material 3.6).

EEG results: spatiotemporal clusters of medial frontal negativity

Significant spatiotemporal clusters were observed for the SRL versus NSRL comparison in all groups. As expected, healthy controls showed MFN modulation in a significant frontal cluster ($t\text{-sum} = -37180.09$, $P = 0.001$), with more negative modulation during the SRL than the NSRL condition. Participants with bvFTD presented no frontal modulation by condition, but they exhibited a small significant posterior (occipital) cluster ($t\text{-sum} = -4700.34$, $P = 0.003$) with more negative voltage during social condition and maximum *t*-value soon after stimulus onset (170 ms). Conversely, the

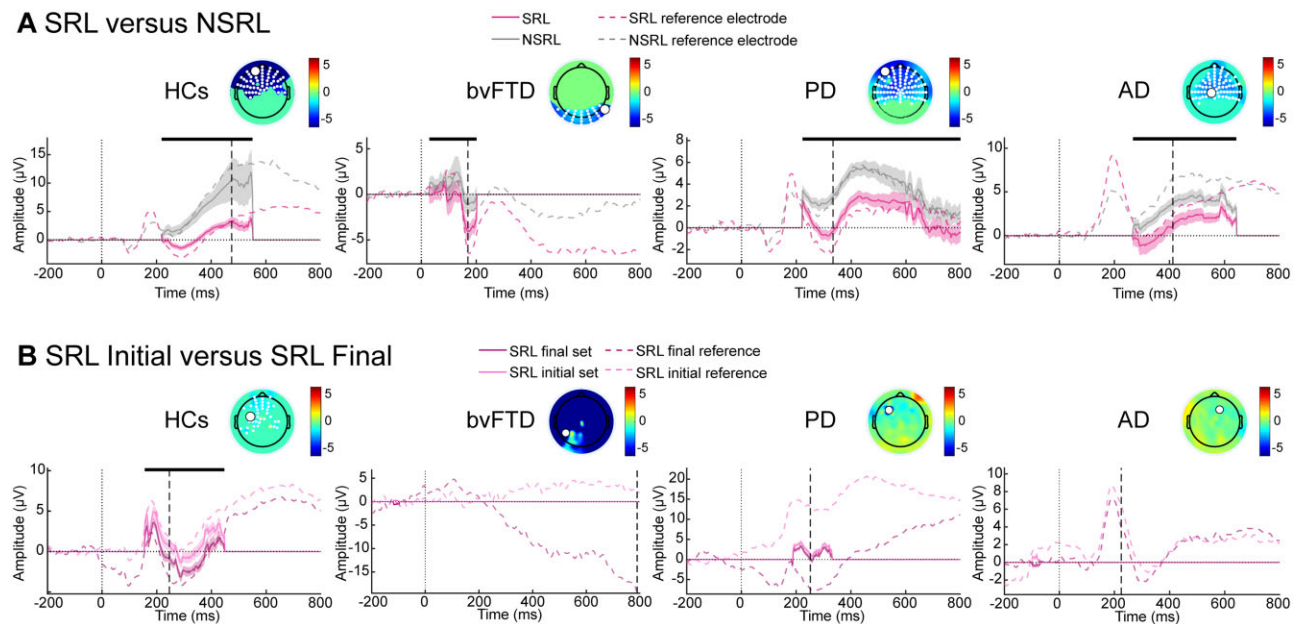


Figure 2 Spatiotemporal cluster results for SRL. (A) SRL versus NSRL conditions for each group. Pink and grey solid curves show the average values of the maximum cluster, while pink and grey dashed curves show the average values of a reference electrode yielding maximum difference by univariate t-test. (B) Initial set versus final set comparison in the SRL condition. Dark pink and light pink solid curves show the average values of the maximum cluster, while dark pink and light pink dashed curves show the average values of a reference electrode yielding maximum difference by univariate t-test. Shaded bars around solid curves indicate SEM. Scalp plots show, for significant clusters, the t-values obtained at time marked by the black vertical dashed line for the electrodes belonging to the cluster (small white dots) and, for the non-significant clusters, the t-values obtained at time marked by the black vertical dashed line for all the electrodes. Black vertical dashed line shows the time when the maximum difference was obtained for the reference electrode (large white black-contoured dot). Black horizontal rectangle indicates time interval where the cluster results are statistically significant. AD = Alzheimer's disease; HCs = healthy controls; PD = Parkinson's disease.

Parkinson's disease group exhibited a significant frontal cluster (t -sum = -87355.85 , $P = 0.001$) in the same direction as healthy controls, with maximum t -value at 334 ms. The Alzheimer's disease group also showed a significant frontal cluster (t -sum = -30859.08 , $P = 0.004$), with more negative voltage for the SRL condition and its maximum t -value at 412 ms (Fig. 2A).

Concerning the effect of learning at neural levels across task cycles, the comparison between initial and final set during the SRL condition was significant for healthy controls (t -sum = -6990.78 , $P = 0.036$), with its maximum t -value at 246 ms, and with an expected more negative voltage (associated with enhanced learning) for the final trials in frontal regions. This effect was not observed in any neurodegenerative group (Fig. 2B).

Neuroimaging results: brain-behaviour associations

When considering all groups, higher performance in SRL was associated with greater volume of temporo-parietal cortices (right superior temporal, supramarginal and postcentral), fronto-limbic regions (right inferior frontal operculum, fusiform and parahippocampal areas; left insula and precentral; bilateral thalamus and middle cingulate areas) and bilateral middle occipital areas (Fig. 3, first row left and Supplementary Table 6.3). Contrarily, higher NSRL performance was associated with greater grey matter volume of the bilateral hippocampus (Fig. 3, first row right and Supplementary Table 6.4).

In the bvFTD group, significant associations emerged between higher performance in SRL and greater volume of predominantly temporo-parietal regions were found (including left superior and middle temporal, bilateral precuneus, fusiform and inferior posterior areas; Fig. 3, second row left and Supplementary Table 6.3). NSRL was associated with greater volume of the right

hippocampus and the middle temporal pole (Fig. 3 second row right and Supplementary Table 6.4).

In the Parkinson's disease group, no significant associations between grey matter volume and performance were found.

The Alzheimer's disease group showed associations between higher SRL performance and greater grey matter volume of predominantly limbic regions (right inferior and superior orbitofrontal, anterior cingulate and hippocampus; left precentral, inferior frontal operculum, insula, middle temporal; and bilateral fusiform—Fig. 3, third row left and Supplementary Table 6.3). NSRL was associated with greater right hippocampus and middle temporal pole grey matter volume (Fig. 3, third row right and Supplementary Table 6.4).

Finally, conjunction analysis of SRL and NSRL conditions (Fig. 4) in all groups revealed small overlapping clusters in the right parahippocampus (peak MNI coordinate: $x = 22.5$; $y = -22.5$; $z = -15$; $k = 292$) and right hypothalamus (peak MNI coordinate: $x = 15$; $y = -4.5$; $z = -10.5$; $k = 224$).

Discussion

We investigated multimodal markers of SRL and NSRL across healthy participants and neurodegenerative diseases. As expected, social feedback enhanced learning in healthy controls. This effect was specifically impaired in bvFTD and Parkinson's disease, while Alzheimer's disease presented generalized learning disruptions. Healthy controls showed the expected pattern of increased MFN modulation during SRL compared to NSRL. This effect was not observed in bvFTD. For SRL learning effects (comparing initial and final cycles of the task), healthy controls exhibited greater MFN modulation for final trials. This MFN differentiation was not seen in any neurodegenerative group. Neuroanatomical correlates of

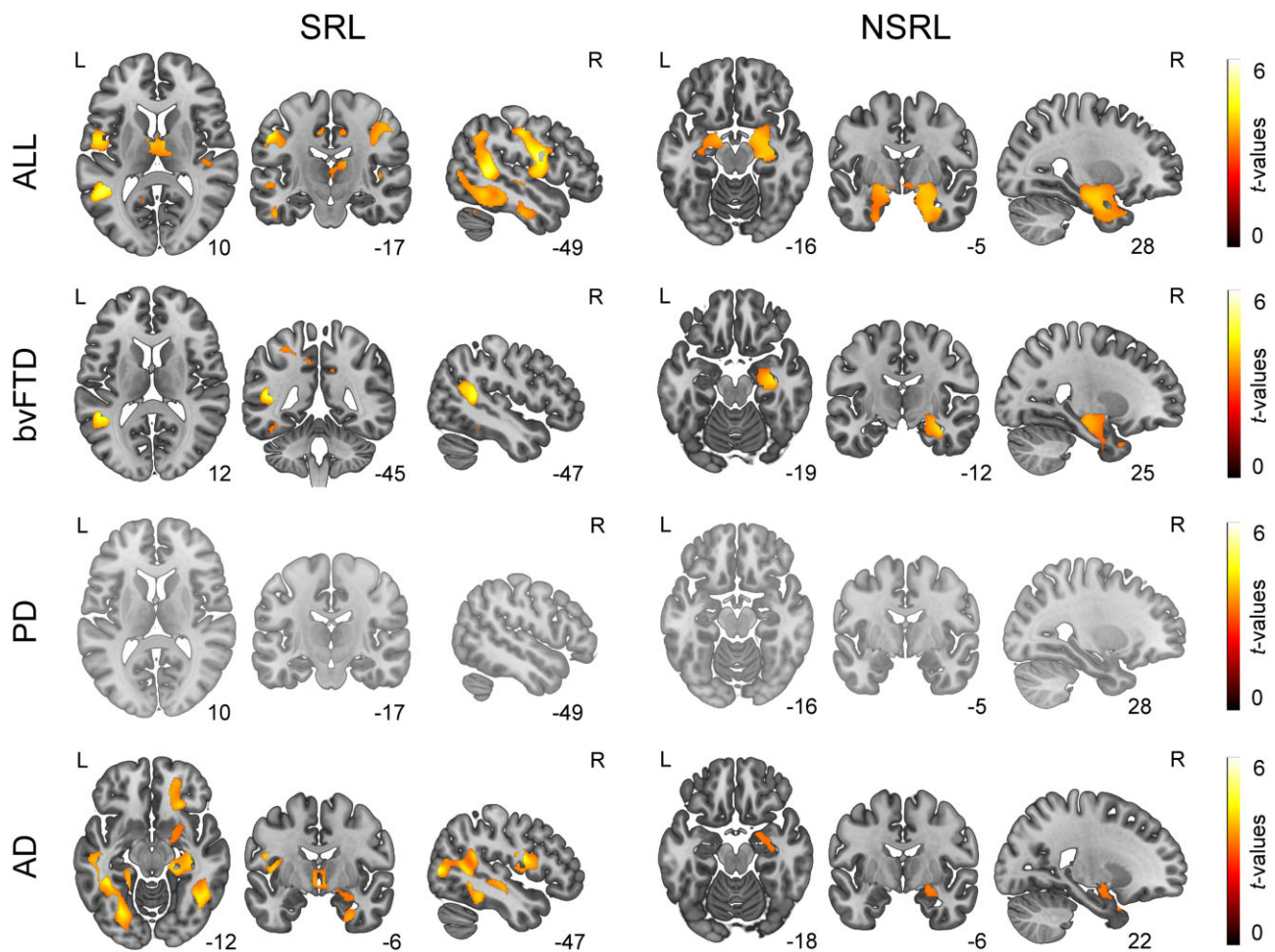


Figure 3 Associations between grey matter volume and SRL/NSRL indexes. These analyses were conducted to identify regions, in all groups together and in separate tandems (bvFTD–healthy controls, PD–healthy controls and AD–healthy controls) associated with SRL and NSRL performance (SnPM, 5000 permutations, cluster-wise inference P-FWE < 0.05). Results are presented on MNI space using the AAL atlas,¹⁶² in the neurological convention. No significant structural associations were found in the PD group. R = right; L = left. AD: Alzheimer’s disease; ALL = all groups; PD = Parkinson’s disease.

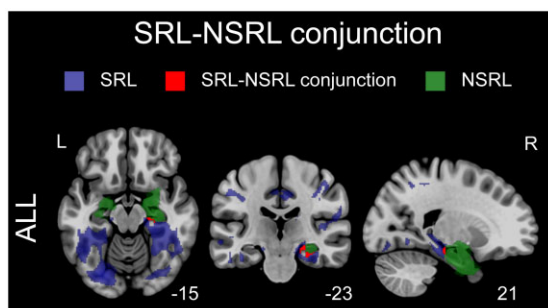


Figure 4 Anatomical conjunction of SRL and NSRL conditions. Whole-brain conjunction analyses were conducted in order to assess the shared and distinct neural correlates of SRL and NSRL conditions. Results are presented on MNI space using the AAL atlas,¹⁶² in neurological convention. Blue represents significant clusters of SRL. Green represents significant clusters of NSRL. Red represents overlapping clusters between SRL and NSRL conditions [right parahippocampus (peak MNI coordinate: x = 22.5; y = -22.5; z = -15; k = 292); and right hypothalamus (peak MNI coordinate: x = 15; y = -4.5; z = -10.5; k = 224)].

SRL showed extended temporo-parietal and fronto-limbic hubs in all groups, as well as associations with specific temporo-parietal regions in bvFTD and predominantly fronto-limbic regions in Alzheimer’s disease. In contrast, NSRL was consistently linked to medial temporal regions and in particular with hippocampus. No association between task performance and brain atrophy was observed in Parkinson’s disease. Together, these multimodal findings reveal mechanisms of learning and social feedback in SRL across different pathophysiological lesion models sensitive to SRL (bvFTD and Parkinson’s disease) and generalized learning deficits (Alzheimer’s disease).

Behavioural social-feedback facilitation and neurodegenerative profiles

The learning gains of healthy controls following social feedback^{10,13} were disrupted in bvFTD and Parkinson’s disease (in their corresponding comparison with controls). While learning from non-social feedback appeared generally unimpaired in these

groups in comparison with controls, the addition of social feedback did not enhance learning. This suggests social cognition deficits impair learning in both diseases,^{40,44} but based on the existing literature, coupled with our novel multimodal imaging findings, there is reason to suspect these deficits may arise from different cognitive processes. In bvFTD, primary social cognitive deficits^{18,36–38,40} may prevent the integration of social information during decision-making processes, disrupting associative learning.^{33,36} This might mirror the way that memory impairments in bvFTD^{47,51,124,134,135} are thought to be explained (in this task) by social cognition deficits. Interestingly, in Parkinson's disease, the interaction of feedback-based learning⁴¹ and socioemotional deficits⁴⁴ (particularly facial processing)⁴⁶ may explain this group's selective SRL disruptions. These potential explanations of behavioural deficits pointing to different physiopathological processes seems to be supported by their brain temporal and spatial signatures (see below). In contrast to these diseases, the generalized impairments across both feedback conditions observed in Alzheimer's disease are likely explained by domain-general associative learning decline¹³⁶ and object memory alterations.^{137,138} Both processes may prevent the integration and maintenance of relevant feedback information. Altogether, behavioural findings parallel clinical patterns of social (bvFTD and Parkinson's disease) and associative learning (Alzheimer's disease) disruptions.

Ongoing cortical correlates of SRL as bvFTD specific markers

Online MFN modulations evidenced both correlates of learning^{53,56,57} and social-feedback facilitation in HCs^{58,139,140} (but see Beston *et al.*³⁵). The selective abolishment on social MFN modulations in bvFTD in comparison with controls, beyond preserved low-level distinction of facial stimulus processing (posterior cluster resembling learning-unrelated N170),¹⁴¹ may be indicative of specific alterations in social prediction-error signal coding. Abnormal social processing may impact action-reward and contextual updating.¹⁴² Indeed, social predictive-error coding is partially indexed by fronto-cingulate mechanisms,¹⁴² compromised in patients with bvFTD. In contrast, altered learning MFN modulations in Parkinson's disease, compatible with fronto-striatal disruptions,¹⁴³ may evidence subtle pathophysiological mechanisms of feedback-related learning deficits. In Alzheimer's disease, disrupted learning MFN modulations¹⁴⁴ may resemble generalized associative learning alterations^{136,137} in accordance with our hypothesis. Thus, the MFN may be considered a novel ongoing marker of SRL in neurodegeneration, selectively compromised in bvFTD.

Neuroanatomical markers of SRL and atrophy mechanisms

Neuroanatomical correlates of SRL suggest that the integration of social and learning processes critically relies on temporo-parietal hubs (i.e. temporo-parietal junction)²⁴ and secondarily on fronto-insular-limbic regions, consistent with predictions from the social-context network model.^{17–22} These hubs index critical processes for socio-contextual learning,¹⁴⁵ including perspective taking, facial emotional recognition, contextual integration, reward processing and object memory. In bvFTD, neuroanatomical signatures of SRL support the role of the temporo-parietal junction in processing behaviourally relevant social information.¹⁴⁶ Perspective taking in socially motivated contexts may also contribute to associative learning and object memory processes.³⁶ Conversely, in Alzheimer's disease, specific limbic involvement in SRL suggests its role in the use of social cues during associative learning. In

particular, associations with hippocampal regions may reflect the involvement of general associative learning and object memory processes.¹⁴⁷ Moreover, additional associations with orbitofrontal, insular, and anterior cingulate regions may indicate socioemotional and reward-related processing.^{22,145,148–150} Lack of neuroanatomical associations in Parkinson's disease suggests specific SRL deficits may be explained by pathophysiological mechanisms unrelated with brain atrophy.¹⁴³

Compared with SRL, NSRL was consistently associated with medial temporal (hippocampal) regions^{6,59} in healthy controls, bvFTD and Alzheimer's disease. In this sense, conjunction analysis suggests large differential anatomical correlates for social and non-social conditions, with minimum overlap. Expected regions involved in general associative and implicit learning such as hippocampus^{151,152} and hypothalamus¹⁵³ evidenced common neural correlates for both social and non-social learning. In sum, cortical temporo-parietal hubs (and, to a lesser extent, fronto-limbic regions) may play a key role in SRL and in selective bvFTD deficits.

Multimodal evidence of distinct mechanisms across neurodegenerative disorders

Our study provides novel multimodal evidence of distinct social and learning processes in neurodegenerative diseases. Ongoing frontal EEG markers and brain structural correlates, captured by the social context network model, shed light on how similar SRL deficits in different diseases may be rooted in distinct anatomofunctional disruptions. Neurophysiological evidence of broad temporo-parietal and frontal involvement in the SRL condition compared to NSRL points to the complexity of social sources of feedback. Results from bvFTD patients, in comparison with controls, reveal selective social deficits consistent across dimensions. Their failure to use socially relevant information as a prior to correct inferential prediction errors and improve learning^{18,39,40} might be related to both neurodegeneration and a lack of appropriate MFN modulations. This lack of social reward mediation in updating expectations and actions could hardly be explained by a perceptual impairment, because visuo-perceptual integration of stimuli seems to be preserved (supported by N170 component modulation¹⁵⁴ and SRL deficits when covarying by valence recognition). Consistent with our findings, prior research has shown that social signals are encoded by the temporo-parietal junction, anterior cingulate and dorsomedial prefrontal cortices.^{24,142} Although future research is needed to test this conjecture, our findings in bvFTD could be explained by alterations in social prediction-error coding. Moreover, these deficits likely exacerbate memory impairments also present in this condition.^{47,51,134,135} Deficits in Parkinson's disease were accompanied by preserved social MFN and impaired learning MFN modulations, as well as a lack of neuroanatomical specificity, suggesting a different pathophysiological mechanism. Specifically, possible MFN-related fronto-striatal dysregulations¹⁴³ may impact social reward prediction-error signals during feedback-related learning.^{3,26,155} Finally, social MFN modulations and fronto-limbic associations in Alzheimer's disease could be impacted by disrupted associative learning and object memory processes in SRL. These mechanisms are strongly affected by medial temporal and temporo-parietal degeneration.¹⁵⁶ Consequently, social-feedback learning facilitation may be vulnerable to decay with increasing disease severity.³⁶ Between-condition comparisons in each neurodegenerative group fall outside the scope of our study. However, multidimensional results coupled with supplementary discussion analysis between conditions among neurodegenerative cases (see [Supplementary material](#) for details) partially support the interpretation of

different social and learning mechanisms, pointing to more specific SRL disruptions in bvFTD.

This convergent evidence of SRL patterns across neurodegenerative diseases carries clinical implications. Social cognitive disruptions and memory alterations have been largely described as canonical deficits in bvFTD and Alzheimer's disease, respectively. However, evidence of memory impairments in bvFTD⁴⁹ and social cognitive deficits in Alzheimer's disease⁵⁰ has hindered differential diagnosis between both conditions.^{47,51} Here we shed light on this issue by combining social cognition and learning processes in a single task, and using multiple levels of analysis including EEG and MRI. Our multimodal findings present two disrupted SRL patterns in bvFTD and Alzheimer's disease. Moreover, they revealed how similar behavioural SRL outcomes (i.e. in bvFTD and Parkinson's disease) may be explained by different neurophysiological pathways. Our study acknowledges the synergic assessment of these cognitive processes^{19–22,157} as well as the specificities of each model in their comparison to healthy controls, offering new transnosological insights across neurodegenerative conditions.

Limitations and further research

We acknowledge certain limitations to our study. First, our design is based on a modest sample size. Nevertheless, it is similar to or larger than those of other multimodal reports assessing neurodegenerative subtypes.^{30,32,36,40,158,159} Also, this caveat was counteracted by the strict control of demographic and clinical variables, as well as detailed diagnostic procedures and systematic assessments. Moreover, our multimodal results across behavioural, electrophysiological and neuroanatomical dimensions, with moderate to large effect sizes, further attests to their robustness. In any case, future studies should replicate and extend these results with larger and adequately matched patient groups and alternative designs allowing for exploration of systematic effects across different neurodegenerative groups. Such an approach may allow for direct patients' group comparisons which are beyond the scope of our study. Second, our findings rely on social-feedback facilitation processes triggered by static emotional faces. Performance was assessed through implicit associations including simple stimuli (three-digit numbers) to prevent semantic confounds and task-load effects on learning outcomes.^{160,161} The use of simple stimuli allows assessing cognitively impaired populations. Notwithstanding, future tasks should strive for greater ecological validity by addressing SRL using more naturalistic settings^{33,34} and stimuli (such as sentences or object localization associations). Third, the processing of socioemotional stimuli in the SRL may be affected by facial emotion recognition disturbances that are characteristic of bvFTD.^{108,109} However, we used a single face displaying only two emotions and our results persisted when controlling for valence recognition ([Supplementary material](#)). These results suggest that feedback processing is influenced by social content (rather than emotional detection impairments). Future studies should compare how learning is affected by different social stimuli (facial versus non-facial and emotional versus non-emotional). In this sense, learning effects between conditions may be influenced by visuo-perceptual complexity of feedback cues. However, several reasons suggest that the observed effects are better explained by the social nature of the SRL stimulus including the robustness of an already validated task¹⁰ similar to previous experimental designs,^{6,33,38} cognitive load control with the use of one face per valence,³⁵ MFN modulations suggesting processing of learning effects instead to stimulus complexity (except for bvFTD), and replication of results after controlling for valence recognition ([Supplementary material](#)). Nonetheless, visuo-perceptual complexity among stimuli should be

better controlled in future works, with a 2×2 (social/non-social, complex/simple) stimuli design. Finally, although our multimodal assessment approach includes task-related EEG measures, future studies should also include active functional neuroimaging paradigms to better elucidate the regions and networks mediating SRL.

Conclusions

Our multimodal lesion model approach reveals convergent evidence of dissociable effects of learning and social feedback across neurodegenerative diseases. These novel results may support theoretical accounts of multimodal SRL mechanisms involving ongoing MFN activity and anatomical deficits underpinned by the social-context network model. A novel clinical agenda is thus opened, related to the characterization and treatment of these social cognition and learning processes in neurodegeneration.

Acknowledgements

We thankfully acknowledge the collaboration of Instituto Conci Carpinella (Córdoba, Argentina) and Hospital Nacional de Clínicas (Facultad de Ciencias Médicas, Universidad Nacional de Córdoba, Córdoba, Argentina). Finally, we thank the participants and their families for their invaluable time and commitment to our study.

Funding

This work is partially supported by grants from Takeda CW2680521; CONICET; ANID/FONDECYT Regular (1210195 and 1210176); FONCYT-PICT 2017–1820; ANID/FONDAP/15150012; Sistema General de Regalías (BPIN2018000100059), Universidad del Valle (CI 5316); Programa Interdisciplinario de Investigación Experimental en Comunicación y Cognición (PIIECC), Facultad de Humanidades, USACH; Alzheimer's Association GBHI ALZ UK-20-639295; and the MULTI-PARTNER CONSORTIUM TO EXPAND DEMENTIA RESEARCH IN LATIN AMERICA [ReDLat, supported by National Institutes of Health, National Institutes of Aging (R01 AG057234), Alzheimer's Association (SG-20-725707), Rainwater Charitable foundation—Tau Consortium, and Global Brain Health Institute)]. The contents of this publication are solely the responsibility of the authors and do not represent the official views of these Institutions.

Competing interests

The authors report no competing interests.

Supplementary material

[Supplementary material](#) is available at *Brain* online.

References

1. Martin J, Rychlowska M, Wood A, Niedenthal P. Smiles as multipurpose social signals. *Trends Cogn Sci*. 2017;21(11):864–877.
2. Verneti A, Smith TJ, Senju A. Gaze-contingent reinforcement learning reveals incentive value of social signals in young children and adults. *Proc R Soc B*. 2017;284(1850):20162747.
3. Kruppa JA, Gossen A, Weiß EO, et al. Neural modulation of social reinforcement learning by intranasal oxytocin in male adults with high-functioning autism spectrum disorder: A randomized trial. *Neuropsychopharmacology*. 2019; 44(4):749–756.

4. Zaki J, Kallman S, Wimmer GE, Ochsner K, Shohamy D. Social cognition as reinforcement learning: Feedback modulates emotion inference. *J Cogn Neurosci*. 2016;28(9):1270–1282.
5. Lin A, Adolphs R, Rangel A. Impaired learning of social compared to monetary rewards in autism. *Front Neurosci*. 2012;6:143.
6. Mihov Y, Mayer S, Musshoff F, Maier W, Kendrick KM, Hurlemann R. Facilitation of learning by social–emotional feedback in humans is beta-noradrenergic-dependent. *Neuropsychologia*. 2010;48(10):3168–3172.
7. Colombo M, Stankevicius A, Seriès P. Benefits of social vs. non-social feedback on learning and generosity. Results from the Tipping Game. *Front Psychol*. 2014;5:1154.
8. Lee J, Green MF. Social preference and glutamatergic dysfunction: Underappreciated prerequisites for social dysfunction in schizophrenia. *Trends Neurosci*. 2016;39(9):587–596.
9. Heerey EA. Learning from social rewards predicts individual differences in self-reported social ability. *J Exp Psychol Gen*. 2014;143(1):332–339.
10. Hurlemann R, Patin A, Onur OA, et al. Oxytocin enhances amygdala-dependent, socially reinforced learning and emotional empathy in humans. *J Neurosci*. 2010;30(14):4999–5007.
11. Olsson A, Phelps EA. Social learning of fear. *Nat Neurosci*. 2007;10(9):1095–1102.
12. Gariépy J-F, Watson KK, Du E, et al. Social learning in humans and other animals. *Front Neurosci*. 2014;8:58.
13. Ferdinand NK, Hilz M. Emotional feedback ameliorates older adults' feedback-induced learning. *PLoS One*. 2020;15(4):e0231964.
14. Fareri DS, Delgado MR. Social rewards and social networks in the human brain. *Neuroscientist*. 2014;20(4):387–402.
15. LaBar KS, Cabeza R. Cognitive neuroscience of emotional memory. *Nat Rev Neurosci*. 2006;7(1):54–64.
16. Tyng CM, Amin HU, Saad MN, Malik AS. The influences of emotion on learning and memory. *Front Psychol*. 2017;8:1454.
17. Baez S, García AM, Ibanez A. The social context network model in psychiatric and neurological diseases. In: *Social behavior from rodents to humans*. Springer; 2016: 379–396.
18. Ibanez A, Manes F. Contextual social cognition and the behavioral variant of frontotemporal dementia. *Neurology*. 2012;78(17):1354–1362.
19. Ibáñez A, García AM. *Contextual cognition: The sensus communis of a situated mind*. Springer; 2018.
20. Ibáñez A. Brain oscillations, inhibition and social inappropriateness in frontotemporal degeneration. *Brain*. 2018;141(10):e73.
21. Ibáñez A, Billeke P, de la Fuente L, Salamone P, García AM, Melloni M. Reply: Towards a neurocomputational account of social dysfunction in neurodegenerative disease. *Brain*. 2017;140(3):e15.
22. Ibanez A, Schulte M. Situated minds: Conceptual and emotional blending in neurodegeneration and beyond. *Brain*. 2020;143(12):3523–3525.
23. Decety J, Lamm C. The role of the right temporoparietal junction in social interaction: How low-level computational processes contribute to meta-cognition. *Neuroscientist*. 2007;13(6):580–593.
24. Joiner J, Piva M, Turrin C, Chang SW. Social learning through prediction error in the brain. *NPJ Sci Learn*. 2017;2(1):8–9.
25. Hu J, Qi S, Becker B, et al. Oxytocin selectively facilitates learning with social feedback and increases activity and functional connectivity in emotional memory and reward processing regions. *Hum Brain Mapp*. 2015;36(6):2132–2146.
26. Lin A, Adolphs R, Rangel A. Social and monetary reward learning engage overlapping neural substrates. *Soc Cogn Affect Neurosci*. 2012;7(3):274–281.
27. Evans S, Fleming SM, Dolan RJ, Averbeck BB. Effects of emotional preferences on value-based decision-making are mediated by mentalizing and not reward networks. *J Cogn Neurosci*. 2011;23(9):2197–2210.
28. Rorden C, Karnath HO. Using human brain lesions to infer function: A relic from a past era in the fMRI age? *Nat Rev Neurosci*. 2004;5(10):813–819.
29. Baez S, Couto B, Torralva T, et al. Comparing moral judgments of patients with frontotemporal dementia and frontal stroke. *JAMA Neurol*. 2014;71(9):1172–1176.
30. García-Cordero I, Sedeño L, de la Fuente L, et al. Feeling, learning from and being aware of inner states: Interoceptive dimensions in neurodegeneration and stroke. *Philos Trans R Soc Lond B Biol Sci*. 2016;371(1708):20160006.
31. Garcia-Cordero I, Sedeño L, Fraiman D, et al. Stroke and neurodegeneration induce different connectivity aberrations in the insula. *Stroke*. 2015;46(9):2673–2677.
32. Salamone PC, Legaz A, Sedeño L, et al. Interoception primes emotional processing: Multimodal evidence from neurodegeneration. *J Neurosci*. 2021;41(19):4276–4292.
33. Keri S. Social influence on associative learning: Double dissociation in high-functioning autism, early-stage behavioural variant frontotemporal dementia and Alzheimer's disease. *Cortex*. 2014;54:200–209.
34. Duff MC, Gallegos DR, Cohen NJ, Tranel D. Learning in Alzheimer's disease is facilitated by social interaction. *J Comp Neurol*. 2013;521(18):4356–4369.
35. Beston PJ, Barbet C, Heerey EA, Thierry G. Social feedback interferes with implicit rule learning: Evidence from event-related brain potentials. *Cogn Affect Behav Neurosci*. 2018;18(6):1248–1258.
36. Wong S, Irish M, O'Callaghan C, et al. Should I trust you? Learning and memory of social interactions in dementia. *Neuropsychologia*. 2017;104:157–167.
37. Kumfor F, Irish M, Hodges JR, Piguet O. The orbitofrontal cortex is involved in emotional enhancement of memory: Evidence from the dementias. *Brain*. 2013;136(Pt 10):2992–3003.
38. Perry DC, Sturm VE, Wood KA, Miller BL, Kramer JH. Divergent processing of monetary and social reward in behavioral variant frontotemporal dementia and Alzheimer's disease. *Alzheimer Dis Assoc Disord*. 2015;29(2):161–164.
39. O'Callaghan C, Bertoux M, Irish M, et al. Fair play: Social norm compliance failures in behavioural variant frontotemporal dementia. *Brain*. 2016;139(Pt 1):204–216.
40. Melloni M, Billeke P, Baez S, et al. Your perspective and my benefit: Multiple lesion models of self–other integration strategies during social bargaining. *Brain*. 2016;139(11):3022–3019.
41. Meissner SN, Südmeyer M, Keitel A, Pollok B, Bellebaum C. Facilitating effects of deep brain stimulation on feedback learning in Parkinson's disease. *Behav Brain Res*. 2016;313:88–96.
42. Schmitt-Eliassen J, Ferstl R, Wiesner C, Deuschl G, Witt K. Feedback-based versus observational classification learning in healthy aging and Parkinson's disease. *Brain Res*. 2007;1142:178–188.
43. Shohamy D, Myers C, Grossman S, Sage J, Gluck M, Poldrack R. Cortico-striatal contributions to feedback-based learning: Converging data from neuroimaging and neuropsychology. *Brain*. 2004;127(Pt 4):851–859.
44. Argaud S, Vérin M, Sauleau P, Grandjean D. Facial emotion recognition in Parkinson's disease: A review and new hypotheses. *Mov Disord*. 2018;33(4):554–567.
45. Baez S, Herrera E, Trujillo C, et al. Classifying Parkinson's disease patients with syntactic and socio-emotional verbal measures. *Front Aging Neurosci*. 2020;12:586233.

46. Ho MW-R, Chien SH-L, Lu M-K, et al. Impairments in face discrimination and emotion recognition are related to aging and cognitive dysfunctions in Parkinson's disease with dementia. *Sci Rep*. 2020;10(1):1–8.
47. Bertoux M, de Souza L, O'Callaghan C, et al. Social cognition deficits: The key to discriminate behavioral variant frontotemporal dementia from Alzheimer's disease regardless of amnesia? *J Alzheimer's Dis*. 2016;49(4):1065–1074.
48. Shany-Ur T, Rankin KP. Personality and social cognition in neurodegenerative disease. *Curr Opin Neurol*. 2011;24(6):550–555.
49. Bertoux M, Flanagan EC, Hobbs M, et al. Structural anatomical investigation of long-term memory deficit in behavioral frontotemporal dementia. *J Alzheimer's Dis*. 2018;62(4):1887–1900.doi:10.3233/jad-170771
50. Strikwerda-Brown C, Ramanan S, Irish M. Neurocognitive mechanisms of theory of mind impairment in neurodegeneration: A transdiagnostic approach. *Neuropsychiatr Dis Treat*. 2019;15:557–573.
51. Hornberger M, Piguet O. Episodic memory in frontotemporal dementia: A critical review. *Brain*. 2012;135(Pt 3):678–692.
52. Seeley WW, Allman JM, Carlin DA, et al. Divergent social functioning in behavioral variant frontotemporal dementia and Alzheimer disease: Reciprocal networks and neuronal evolution. *Alzheimer Dis Assoc Disord*. 2007;21(4):S50–S57.
53. Van Der Helden J, Boksem MA. Medial frontal negativity reflects learning from positive feedback. *Psychophysiology*. 2012;49(8):1109–1113.
54. Van Noordt SJ, Campopiano A, Segalowitz SJ. A functional classification of medial frontal negativity ERPs: Theta oscillations and single subject effects. *Psychophysiology*. 2016;53(9):1317–1334.
55. Yeung N, Sanfey AG. Independent coding of reward magnitude and valence in the human brain. *J Neurosci*. 2004;24(28):6258–6264.
56. Luft CDB. Learning from feedback: The neural mechanisms of feedback processing facilitating better performance. *Behav Brain Res*. 2014;261:356–368.
57. de Buijn ER, Mars RB, Hester R. Processing of performance errors predicts memory formation: Enhanced feedback-related negativities for corrected versus repeated errors in an associative learning paradigm. *Eur J Neurosci*. 2020;51(3):881–890.
58. Pfabigan DM, Han S. Converging electrophysiological evidence for a processing advantage of social over nonsocial feedback. *Cogn Affect Behav Neurosci*. 2019;19(5):1170–1183.
59. Onur OA, Schlaepfer TE, Kukulja J, et al. The N-methyl-D-aspartate receptor co-agonist D-cycloserine facilitates declarative learning and hippocampal activity in humans. *Biol Psychiatry*. 2010;67(12):1205–1211.
60. Rascovsky K, Hodges JR, Knopman D, et al. Sensitivity of revised diagnostic criteria for the behavioural variant of frontotemporal dementia. *Brain*. 2011;134(Pt 9):2456–2477.
61. Hughes AJ, Daniel SE, Kilford L, Lees AJ. Accuracy of clinical diagnosis of idiopathic Parkinson's disease: A clinico-pathological study of 100 cases. *J Neurol Neurosurg Psychiatry*. 1992;55(3):181–184.
62. Dubois B, Feldman HH, Jacova C, et al. Research criteria for the diagnosis of Alzheimer's disease: Revising the NINCDS-ADRDA criteria. *Lancet Neurol*. 2007;6(8):734–746.
63. McKhann GM, Knopman DS, Chertkow H, et al. The diagnosis of dementia due to Alzheimer's disease: Recommendations from the National Institute on Aging–Alzheimer's Association workgroups on diagnostic guidelines for Alzheimer's disease. *Alzheimer's Dement*. 2011;7(3):263–269.
64. Ibáñez A, Pina-Escudero SD, Possin KL, et al. Dementia caregiving across Latin America and the Caribbean and brain health diplomacy. *Lancet Healthy Longevity*. 2021;2(4):e222–e231.
65. Ibanez A, Yokoyama JS, Possin KL, et al. The multi-partner consortium to expand dementia Research in Latin America (ReDLat): Driving multicentric research and implementation science. *Front Neurol*. 2021;12:631722.
66. Sedeno L, Piguet O, Abrevaya S, et al. Tackling variability: A multicenter study to provide a gold-standard network approach for frontotemporal dementia. *Hum Brain Mapp*. 2017;38(8):3804–3822.
67. Donnelly-Kehoe PA, Pascariello GO, García AM, et al. Robust automated computational approach for classifying frontotemporal neurodegeneration: Multimodal/multicenter neuroimaging. *Alzheimer's Dement (Amst)*. 2019;11(C):588–598.
68. Baez S, Manes F, Huepe D, et al. Primary empathy deficits in frontotemporal dementia. *Front Aging Neurosci*. 2014;6:262.
69. Moguilner S, García AM, Perl YS, et al. Dynamic brain fluctuations outperform connectivity measures and mirror pathophysiological profiles across dementia subtypes: A multicenter study. *Neuroimage*. 2021;225:117522.
70. Ibáñez A, Fittipaldi S, Trujillo C, et al. Predicting and characterizing neurodegenerative subtypes with multimodal neurocognitive signatures of social and cognitive processes. *J Alzheimer's Dis*. 2021;83(1):227–248.
71. Piguet O, Hornberger M, Mioshi E, Hodges JR. Behavioural-variant frontotemporal dementia: Diagnosis, clinical staging, and management. *Lancet Neurol*. 2011;10(2):162–172.
72. Whitwell JL, Przybelski SA, Weigand SD, et al. Distinct anatomical subtypes of the behavioural variant of frontotemporal dementia: A cluster analysis study. *Brain*. 2009;132(11):2932–2946.
73. Huber SJ, Shuttleworth EC, Christy JA, Chakeres DW, Curtin A, Paulson GW. Magnetic resonance imaging in dementia of Parkinson's disease. *J Neurol Neurosurg Psychiatry*. 1989;52(11):1221–1227.
74. Schulz JB, Skalej M, Wedekind D, et al. Magnetic resonance imaging-based volumetry differentiates idiopathic Parkinson's syndrome from multiple system atrophy and progressive supranuclear palsy. *Ann Neurol*. 1999;45(1):65–74.
75. Price S, Paviour D, Scahill R, et al. Voxel-based morphometry detects patterns of atrophy that help differentiate progressive supranuclear palsy and Parkinson's disease. *Neuroimage*. 2004;23(2):663–669.
76. Du A-T, Schuff N, Kramer JH, et al. Different regional patterns of cortical thinning in Alzheimer's disease and frontotemporal dementia. *Brain*. 2006;130(4):1159–1166.
77. Pini L, Pievani M, Bocchetta M, et al. Brain atrophy in Alzheimer's disease and aging. *Ageing Res Rev*. 2016;30:25–48.
78. Landin-Romero R, Kumfor F, Leyton CE, Irish M, Hodges JR, Piguet O. Disease-specific patterns of cortical and subcortical degeneration in a longitudinal study of Alzheimer's disease and behavioural-variant frontotemporal dementia. *Neuroimage*. 2017;151:72–80.
79. Kim D, Kim S-K. Comparing patterns of component loadings: Principal Component Analysis (PCA) versus Independent Component Analysis (ICA) in analyzing multivariate non-normal data. *Behav Res Methods*. 2012;44(4):1239–1243.
80. Pollatos O, Schandry R. Accuracy of heartbeat perception is reflected in the amplitude of the heartbeat-evoked brain potential. *Psychophysiology*. 2004;41(3):476–482.
81. Terhaar J, Viola FC, Bar KJ, Debener S. Heartbeat evoked potentials mirror altered body perception in depressed patients. *Clin Neurophysiol*. 2012;123(10):1950–1957.
82. Schandry R, Montoya P. Event-related brain potentials and the processing of cardiac activity. Research Support, Non-U.S. Gov't. *Biol Psychol*. 1996;42(1-2):75–85.

83. Salamone PC, Esteves S, Sinay VJ, et al. Altered neural signatures of interoception in multiple sclerosis. *Hum Brain Mapp.* 2018;39(12):4743–4754.
84. Garcia-Cordero I, Esteves S, Mikulan EP, et al. Attention, in and out: Scalp-level and intracranial EEG correlates of interoception and exteroception. *Front Neurosci.* 2017;11:411.
85. Yoris A, Abrevaya S, Esteves S, et al. Multilevel convergence of interoceptive impairments in hypertension: New evidence of disrupted body-brain interactions. *Hum Brain Mapp.* 2018;39(4):1563–1581.
86. Dirlich G, Vogl L, Plaschke M, Strian F. Cardiac field effects on the EEG. *Electroencephalogr Clin Neurophysiol.* 1997;102(4):307–315.
87. Yoris A, Garcia AM, Traiber L, et al. The inner world of overactive monitoring: Neural markers of interoception in obsessive-compulsive disorder. *Psychol Med.* 2017;47(11):1957–1970.
88. Zich C, Debener S, Kranczioch C, Bleichner MG, Gutberlet I, De Vos M. Real-time EEG feedback during simultaneous EEG-fMRI identifies the cortical signature of motor imagery. *Neuroimage.* 2015;114:438–447.
89. Nichols TE, Das S, Eickhoff SB, et al. Best practices in data analysis and sharing in neuroimaging using MRI. *Nat Neurosci.* 2017;20(3):299–303.
90. Poldrack RA, Baker CI, Durnez J, et al. Scanning the horizon: Towards transparent and reproducible neuroimaging research. *Nat Rev Neurosci.* 2017;18(2):115–126.
91. Gonzalez CC, Salamone P, Rodríguez-Arriagada N, et al. Fatigue in multiple sclerosis is associated with multimodal interoceptive abnormalities. *Multiple Scler J.* 2019;1352458519888881.
92. Ashburner J, Friston KJ. Voxel-based morphometry—The methods. *Neuroimage.* 2000;11(6 Pt 1):805–821.
93. Ashburner J. A fast diffeomorphic image registration algorithm. *Neuroimage.* 2007;38(1):95–113.
94. Burton EJ, McKeith IG, Burn DJ, Williams ED, O'Brien JT. Cerebral atrophy in Parkinson's disease with and without dementia: A comparison with Alzheimer's disease, dementia with Lewy bodies and controls. *Brain.* 2004;127(Pt 4):791–800.
95. Jack CR, Petersen RC, Xu YC, et al. Medial temporal atrophy on MRI in normal aging and very mild Alzheimer's disease. *Neurology.* 1997;49(3):786–794.
96. La Joie R, Perrotin A, Barré L, et al. Region-specific hierarchy between atrophy, hypometabolism, and β -amyloid (A β) load in Alzheimer's disease dementia. *J Neurosci.* 2012;32(46):16265–16273.
97. van Loenhoud AC, Wink AM, Groot C, et al. A neuroimaging approach to capture cognitive reserve: Application to Alzheimer's disease. *Hum Brain Mapp.* 2017;38(9):4703–4715.
98. Chung J, Yoo K, Lee P, et al. Normalization of cortical thickness measurements across different T1 magnetic resonance imaging protocols by novel W-Score standardization. *Neuroimage.* 2017;159:224–235.
99. Ossenkoppele R, Pijnenburg YA, Perry DC, et al. The behavioural/dysexecutive variant of Alzheimer's disease: Clinical, neuroimaging and pathological features. *Brain.* 2015;138(9):2732–2749.
100. Zimmerman DW. Increasing the power of nonparametric tests by detecting and downweighting outliers. *J Exp Educ.* 1995;64(1):71–78.
101. Zamorano F, Billeke P, Kausel L, et al. Lateral prefrontal activity as a compensatory strategy for deficits of cortical processing in Attention Deficit Hyperactivity Disorder. *Sci Rep.* 2017;7(1):7181.
102. Billeke P, Armijo A, Castillo D, et al. Paradoxical expectation: Oscillatory brain activity reveals social interaction impairment in schizophrenia. *Biol Psychiatry.* 2015;78(6):421–431.
103. Zamorano F, Billeke P, Hurtado J, et al. Temporal constraints of behavioral inhibition: Relevance of inter-stimulus interval in a Go–Nogo task. *PLoS One.* 2014;9(1):e87232.
104. Shany-Ur T, Lin N, Rosen HJ, Sollberger M, Miller BL, Rankin KP. Self-awareness in neurodegenerative disease relies on neural structures mediating reward-driven attention. *Brain.* 2014;137(Pt 8):2368–2381.
105. Chiong W, Wood KA, Beagle AJ, et al. Neuroeconomic dissociation of semantic dementia and behavioural variant frontotemporal dementia. *Brain.* 2016;139(2):578–587.
106. Garcia-Cordero I, Sedeño L, Babino A, et al. Explicit and implicit monitoring in neurodegeneration and stroke. *Sci Rep.* 2019;9(1):14032–14010.
107. Langella S, Sadiq MU, Mucha PJ, Giovanello KS, Dayan E.; Alzheimer's Disease Neuroimaging Initiative. Lower functional hippocampal redundancy in mild cognitive impairment. *Transl Psychiatry.* 2021;11(1):61.
108. Kumfor F, Ibañez A, Hutchings R, Hazelton JL, Hodges JR, Piguet O. Beyond the face: How context modulates emotion processing in frontotemporal dementia subtypes. *Brain.* 2018;141(4):1172–1185.
109. Kumfor F, Irish M, Hodges JR, Piguet O. Discrete neural correlates for the recognition of negative emotions: Insights from frontotemporal dementia. *PLoS One.* 2013;8(6):e67457.
110. Crawford JR, Garthwaite PH, Porter S. Point and interval estimates of effect sizes for the case-controls design in neuropsychology: Rationale, methods, implementations, and proposed reporting standards. *Cogn Neuropsychol.* 2010;27(3):245–260.
111. Voegler R, Peterburs J, Bellebaum C, Straube T. Modulation of feedback processing by social context in social anxiety disorder (SAD)—An event-related potentials (ERPs) study. *Sci Rep.* 2019;9(1):4795.
112. Boudewyn MA, Luck SJ, Farrens JL, Kappenman ES. How many trials does it take to get a significant ERP effect? It depends. *Psychophysiology.* 2018;55(6):e13049.
113. Clayson PE, Baldwin SA, Larson MJ. How does noise affect amplitude and latency measurement of event-related potentials (ERPs)? A methodological critique and simulation study. *Psychophysiology.* 2013;50(2):174–186.
114. Poulsen C, Luu P, Davey C, Tucker DM. Dynamics of task sets: Evidence from dense-array event-related potentials. *Cogn Brain Res.* 2005;24(1):133–154.
115. Baker E, Veytsman E, Martin AM, Blacher J, Stavropoulos KK. Increased neural reward responsivity in adolescents with ASD after social skills intervention. *Brain Sci.* 2020;10(6):402.
116. Depue BE, Ketz N, Mollison MV, Nyhus E, Banich MT, Curran T. ERPs and neural oscillations during volitional suppression of memory retrieval. *J Cogn Neurosci.* 2013;25(10):1624–1633.
117. Maris E, Oostenveld R. Nonparametric statistical testing of EEG- and MEG-data. *J Neurosci Methods.* 2007;164(1):177–190.
118. Bullmore ET, Suckling J, Overmeyer S, Rabe-Hesketh S, Taylor E, Brammer MJ. Global, voxel, and cluster tests, by theory and permutation, for a difference between two groups of structural MR images of the brain. *IEEE Trans Med Imaging.* 1999;18(1):32–42.
119. Chennu S, Noreika V, Gueorguiev D, et al. Expectation and attention in hierarchical auditory prediction. *J Neurosci.* 2013;33(27):11194–11205.
120. Manly B. *Randomization, bootstrap, and Monte Carlo methods in biology.* 3rd ed. Chapman & Hall; 2007.

121. Nichols TE. Multiple testing corrections, nonparametric methods, and random field theory. *Neuroimage*. 2012;62(2):811–815.
122. Sollberger M, Stanley CM, Wilson SM, et al. Neural basis of interpersonal traits in neurodegenerative diseases. *Neuropsychologia*. 2009;47(13):2812–2827.
123. Irish M, Addis DR, Hodges JR, Piguët O. Considering the role of semantic memory in episodic future thinking: Evidence from semantic dementia. *Brain*. 2012;135(Pt 7):2178–2191.
124. Irish M, Piguët O, Hodges JR, Hornberger M. Common and unique gray matter correlates of episodic memory dysfunction in frontotemporal dementia and Alzheimer's disease. *Hum Brain Mapp*. 2014;35(4):1422–1435.
125. Santamaría-García H, Baez S, Reyes P, et al. A lesion model of envy and Schadenfreude: Legal, deservingness and moral dimensions as revealed by neurodegeneration. *Brain*. 2017;140(12):3357–3377.
126. Garcia-Cordero I, Migeot J, Fittipaldi S, et al. Metacognition of emotion recognition across neurodegenerative diseases. *Cortex*. 2021;137:93–107.
127. Ibañez A, Fittipaldi S, Trujillo C, et al. Predicting and characterizing neurodegenerative subtypes with multimodal neurocognitive signatures of social and cognitive processes. *J Alzheimer's Dis*. 2021;83(1):227–222.
128. Bertoux M, Duclos H, Caillaud M, et al. When affect overlaps with concept: Emotion recognition in semantic variant of primary progressive aphasia. *Brain*. 2020;143(12):3850–3864.
129. Fernández-Cabello S, Kronbichler M, Van Dijk KR, Goodman JA, Spreng RN, Schmitz TW; Alzheimer's Disease Neuroimaging Initiative. Basal forebrain volume reliably predicts the cortical spread of Alzheimer's degeneration. *Brain*. 2020;143(3):993–1009.
130. Han H, Glenn AL, Dawson KJ. Evaluating alternative correction methods for multiple comparison in functional neuroimaging research. *Brain Sci*. 2019;9(8):198.
131. Sankar A, Yttredahl AA, Fourcade EW, et al. Dissociable neural responses to monetary and social gain and loss in women with major depressive disorder. *Front Behav Neurosci*. 2019;13:149.
132. Subramaniam K, Gill J, Slattery P, et al. Neural mechanisms of positive mood induced modulation of reality monitoring. *Front Hum Neurosci*. 2016;10:581.
133. Legaz A. Socially Reinforced Learning in Neurodegeneration—ANID/FONDECYT (1170010). osf.io/9nw8j
134. Kumfor F, Hutchings R, Irish M, et al. Do I know you? Examining face and object memory in frontotemporal dementia. *Neuropsychologia*. 2015;71:101–111.
135. Ramanan S, Bertoux M, Flanagan E, et al. Longitudinal executive function and episodic memory profiles in behavioral-variant frontotemporal dementia and Alzheimer's disease. *J Int Neuropsychol Soc*. 2017;23(1):34–43.
136. Barnett JH, Blackwell AD, Sahakian BJ, Robbins TW. The paired associates learning (PAL) test: 30 years of CANTAB translational neuroscience from laboratory to bedside in dementia research. *Transl Neuropsychopharmacol*. 2015;449–474.
137. Maass A, Berron D, Harrison TM, et al. Alzheimer's pathology targets distinct memory networks in the ageing brain. *Brain*. 2019;142(8):2492–2509.
138. Dermody N, Wong S, Ahmed R, Piguët O, Hodges JR, Irish M. Uncovering the neural bases of cognitive and affective empathy deficits in Alzheimer's disease and the behavioral-variant of frontotemporal dementia. *J Alzheimer's Dis*. 2016;53(3):801–816.
139. Pfabigan DM, Gittenberger M, Lamm C. Social dimension and complexity differentially influence brain responses during feedback processing. *Soc Neurosci*. 2019;14(1):26–40.
140. Shen Q, Zhu L, Meng L, et al. To reveal or not to reveal? Observation of social outcomes facilitates reward processing. *Front Neurosci*. 2020;14:579702.
141. Ibanez A, Melloni M, Huepe D, et al. What event-related potentials (ERPs) bring to social neuroscience? *Soc Neurosci*. 2012;7(6):632–649.
142. Lockwood PL, Klein-Flügge M. Computational modelling of social cognition and behaviour—A reinforcement learning primer. *Soc Cogn Affect Neurosci*. 2020;16(8):761–771.
143. Gratwicke J, Jahanshahi M, Foltynie T. Parkinson's disease dementia: A neural networks perspective. *Brain*. 2015;138(Pt 6):1454–1476.
144. Bertoux M, Delavest M, de Souza LC, et al. Social cognition and emotional assessment differentiates frontotemporal dementia from depression. *J Neurol Neurosurg Psychiatry*. 2012;83(4):411–416.
145. Olsson A, Knapska E, Lindström B. The neural and computational systems of social learning. *Nat Rev Neurosci*. 2020;21(4):197–212.
146. Carter RM, Huettel SA. A nexus model of the temporal-parietal junction. *Trends Cogn Sci*. 2013;17(7):328–336.
147. Rolls ET. Limbic systems for emotion and for memory, but no single limbic system. *Cortex*. 2015;62:119–157.
148. Rolls ET. The cingulate cortex and limbic systems for emotion, action, and memory. *Brain Struct Funct*. 2019;224(9):3001–3018.
149. Apps MA, Rushworth MF, Chang SW. The anterior cingulate gyrus and social cognition: Tracking the motivation of others. *Neuron*. 2016;90(4):692–707.
150. Rudebeck PH, Rich EL. Orbitofrontal cortex. *Curr Biol*. 2018;28(18):R1083–R1088.
151. Spurny B, Seiger R, Moser P, et al. Hippocampal GABA levels correlate with retrieval performance in an associative learning paradigm. *Neuroimage*. 2020;204:116244.
152. Simon JR, Vaidya CJ, Howard JH Jr, Howard D. The effects of aging on the neural basis of implicit associative learning in a probabilistic triplets learning task. *J Cogn Neurosci*. 2012;24(2):451–463.
153. Burdakov D, Peleg-Raibstein D. The hypothalamus as a primary coordinator of memory updating. *Physiol Behav*. 2020;223:112988.
154. Hinojosa J, Mercado F, Carretié L. N170 sensitivity to facial expression: A meta-analysis. *Neurosci Biobehav Rev*. 2015;55:498–509.
155. García-García I, Zeighami Y, Dagher A. Reward prediction errors in drug addiction and Parkinson's disease: From neurophysiology to neuroimaging. *Curr Neurol Neurosci Rep*. 2017;17(6):46.
156. Wikenheiser AM, Marrero-Garcia Y, Schoenbaum G. Suppression of ventral hippocampal output impairs integrated orbitofrontal encoding of task structure. *Neuron*. 2017;95(5):1197–1207.e3.
157. Ibañez A. Insular networks and inter cognition in the wild. *Cortex*. 2019;115:341–344.
158. Moretti L, Dragone D, Di Pellegrino G. Reward and social valuation deficits following ventromedial prefrontal damage. *J Cogn Neurosci*. 2009;21(1):128–140.
159. Hughes LE, Nestor PJ, Hodges JR, Rowe JB. Magnetoencephalography of frontotemporal dementia: Spatiotemporally localized changes during semantic decisions. *Brain*. 2011;134(Pt 9):2513–2522.

160. Chan RC, Shum D, Toulopoulou T, Chen EY. Assessment of executive functions: Review of instruments and identification of critical issues. *Arch Clin Neuropsychol*. 2008;23(2):201–216.
161. Luria R, Sessa P, Gotler A, Jolicœur P, Dell'Acqua R. Visual short-term memory capacity for simple and complex objects. *J Cogn Neurosci*. 2010;22(3):496–512.
162. Tzourio-Mazoyer N, Landeau B, Papathanassiou D, et al. Automated anatomical labeling of activations in SPM using a macroscopic anatomical parcellation of the MNI MRI single-subject brain. *Neuroimage*. 2002;15(1):273–289.
163. Lenhard W, Lenhard A. *Calculation of effect sizes*. Dettelbach; 2016.
164. Nasreddine ZS, Phillips NA, Bédirian V, et al. The Montreal Cognitive Assessment, MoCA: A Brief Screening Tool For Mild Cognitive Impairment. *Journal of the American Geriatrics Society*. 53(4):695–699.